Ocean Science

Open Access

Near-surface measurements of sea spray aerosol production over whitecaps in the open ocean

S. J. Norris[1], I. M. Brooks[1], B. I. Moat[2], M. J. Yelland[2], G. de Leeuw[3,4,5], R. W. Pascal[2], and B. Brooks[1]

[1]School of Earth and Environment, University of Leeds, UK
[2]National Centre of Oceanography, Southampton, UK
[3]Climate Change Unit, Finnish Meteorological Institute, Helsinki, Finland
[4]Department of Physics, University of Helsinki, Helsinki, Finland
[5]Netherlands Organisation for Applied Scientific Research – TNO, Utrecht, The Netherlands

Correspondence to: S. J. Norris (snorris@env.leeds.ac.uk)

Abstract. Simultaneous measurements of near-surface aerosol ($0.12 < R < 9.25\,\mu m$) and bubble spectra ($13 < R < 620\,\mu m$) were made during five buoy deployments in the open ocean of the North Atlantic and used to estimate aerosol fluxes per unit area of whitecap. The measurements were made during two cruises as part of the Sea Spray, Gas Flux, and Whitecaps (SEASAW) project, a UK contribution to the international Surface Ocean Lower Atmosphere Study (SOLAS) program. The mean bubble number concentrations for each deployment are in broad agreement with other open ocean spectra and are consistently one to two orders of magnitude lower than surf zone studies. Production fluxes per unit area of whitecap are estimated from the mean aerosol concentration for each buoy deployment. They are found to increase with wind speed, and span the range of values found by previous laboratory and surf-zone studies for particles with radius at 80 % relative humidity, $R_{80} < 1\,\mu m$, but to drop off more rapidly with increasing particle size for larger particles. Estimates of the mean sea spray flux were made by scaling the whitecap production fluxes with in situ estimates of whitecap fraction. The sea spray fluxes are also compared with simultaneous individual eddy covariance flux estimates, and with a sea spray source function derived from them.

1 Introduction

Sea spray aerosol is an important component of the climate system and the largest single source of aerosol mass injected into the atmosphere after wind-blown dust (Hoppel et al., 2002). Under clear skies over the remote ocean, sea salt aerosol is the dominant scatterer of incoming solar radiation (Haywood et al., 1999); it plays a significant role in controlling the microphysics and chemistry of marine stratocumulus (O'Dowd et al., 1999) and provides a substantial sink for atmospheric trace gases, both natural and anthropogenic (O'Dowd et al., 2000). To quantify the effects of sea spray aerosol on the environment, a detailed knowledge of the numbers and sizes of aerosol particles produced at the ocean surface is required.

There are two production mechanisms for sea spray particles: mechanical tearing of water droplets (spume) from wave crests at high wind speeds, and the bursting of bubbles at the water surface. Bubbles form predominantly from breaking wind waves in the open ocean (Kolovayev, 1976); these entrain air into the near-surface water column producing a plume of bubbles (Blanchard and Woodcock, 1957); as the bubbles rise they form regions of foam at the surface-whitecaps. Other potential production mechanisms for bubbles include production by the respiration of phytoplankton (Medwin, 1970; Johnson and Wangersky, 1987), release from the sea bed (e.g. Leighton and Robb, 2008), gases coming out of solution as gas-saturated water warms (Norris et al., 2011), and where sea ice is present the release of bubbles

trapped in melting ice or expelled during the freezing process (Wettlaufer, 1998).

Bursting bubbles produce droplets by two distinct mechanisms: disintegration of the bubble film produces a large number (100s to 1000s) of droplets smaller than about $R = 2\,\mu m$, while the collapse of the sides of the bubble cavity results in the ejection of a jet of water from the centre of the collapsing bubble, which breaks into a handful of droplets of radii between about 1 and 50 μm. The precise size and number of droplets produced by a single bubble depends on the bubble size (Blanchard, 1983), water properties (Mårtensson et al., 2003) and the presence of surface active material (Morelli et al., 1974; Blanchard, 1990). The smallest bubbles produce only jet droplets, while the largest produce only film droplets; the limits between them are not well defined, however, and depend on the properties of both water and surface microlayer. Day (1964) found a bubble radius of approximately 50 μm to be the minimum size producing film droplets, while Spiel (1997) found the limit to be 600 μm. The largest jet droplet produced by a bubble is roughly 1/10 the radius of the parent bubble (Blanchard, 1963; Spiel, 1994). The upper limit on bubble radius for the production of jet droplets is variously cited to be as low as 450 μm (Blanchard, 1963) and as high as 2.94 mm (Georgescu et al., 2002); this latter value is double the often quoted value of 1.5 mm from Spiel's (1997) experimental study.

Turbulent air motion mixes the ejected droplets upwards, opposed by their gravitational fall speed, resulting in a change in particle spectra with altitude (Monahan, 1968; Wu et al., 1984; de Leeuw, 1989; Parameswaran, 2001). During transport, transformation due to coagulation, evaporation and chemical processes may occur, resulting in high variability in the aerosol's physical and chemical properties. Newly generated sea spray droplets shrink via evaporation until they reach a state of equilibrium with the ambient relative humidity, in contrast to fresh water droplets which evaporate entirely. For ease of comparison aerosol spectra are usually adjusted to a reference humidity – commonly 80 %, with the radius denoted R_{80}. The size of a particle influences its life cycle in the atmosphere. Particles in the nucleation mode ($R_{80} < 0.1\,\mu m$) grow by condensation and coagulation, eventually becoming accumulation mode particles ($0.1 < R_{80} < 5\,\mu m$), which have the longest residence times. For particles with $R_{80} > 10\,\mu m$ an increasing fraction fall back to the surface before reaching equilibrium (Andreas et al., 2010), imposing an upper size limit on the resulting aerosol spectra. Turbulent mixing means that any measured aerosol spectrum will represent a mixture of newly generated with pre-existing aerosol.

Many parameterizations for the sea spray generation function have been proposed, based on a variety of observational techniques (see Lewis and Schwartz, 2004 for an overview). One approach has been to estimate the interfacial production flux per unit area of whitecap and to scale this by the fractional area coverage of whitecaps on the sea surface, W,

in turn often parameterized as a function of the mean local wind speed. It has usually been assumed that the production flux is independent of the nature and extent of the whitecap, including its production mechanism. One of the most commonly used such formulations is that of Monahan and O'Muircheartaigh (1986), which is based on the production flux of particles per unit area of whitecap obtained in a laboratory study (Spiel, 1983) and an empirical relationship for the whitecap fraction as a function of wind speed (Monahan and O'Muircheartaigh, 1980):

$$W = 3.84 \times 10^{-4} U_{10}^{3.41}, \tag{1}$$

where U_{10} is the wind speed at 10 m above the sea surface, and W is in %. There are many different whitecap fraction parameterizations derived from photographs and videos of the sea surface from towers, aircraft, and ships. Anguelova and Webster (2006) provide an extensive summary of many studies, and find that they span a range of approximately 2–3 orders of magnitude at all wind speeds. It is generally recognized that whitecap fraction is zero for wind speeds less than about $3\,m\,s^{-1}$ (Blanchard, 1963; Monahan, 1971).

The production flux of aerosol from a unit area of whitecap has been estimated from laboratory studies (Monahan et al., 1982; Cipriano et al., 1983, 1987; Woolf et al., 1988; Mårtensson et al., 2003; Tyree et al., 2007; Keene et al., 2007; Facchini et al., 2008; Fuentes et al., 2010), though only the study of Mårtensson et al. (2003) is readily comparable with this study, and measurements over natural surf zone whitecaps (Woodcock et al., 1963; Blanchard, 1969; de Leeuw et al., 2000; Clarke et al., 2006). The advantage of laboratory measurements is the ability to control the environmental conditions; however, it is difficult to create conditions truly representative of the open ocean, particularly those of well-developed sea states, mixed seas or high winds. A more representative approach would be to make in situ estimates of the direct aerosol production from whitecaps at sea. However, making measurements in the open ocean close enough to the surface to isolate the aerosol generated by individual whitecaps from the background aerosol is difficult. Historically, optical particle counters have been heavy and physically bulky instruments, which are difficult to locate near the ocean surface. Therefore, the majority of the field measurements of sea spray particle number concentrations have been made 5–25 m above the surface and then interpolated to a reference level for comparison (usually the surface or 10 m above mean surface level) (Andreas, 2002). New technology is now making small, lightweight, and relatively cheap sensors increasingly available (e.g. Hill et al., 2008) enabling measurement approaches that were not previously viable.

De Leeuw et al. (2000) and Clarke et al. (2006) used measurements over surf zone whitecaps to estimate the production of sea spray aerosol. Measuring over the surf zone allows the instruments to be located on solid ground; however, a major concern is the extent to which the surf zone whitecaps are representative of whitecaps in the open ocean.

The size spectra are very different for bubbles larger than about 50 μm radius, and surf zone bubble number concentrations can be two orders of magnitude larger than those in the open ocean (Brooks et al., 2009a). The wave breaking process in the surf zone results from interaction with the sea bed, whereas in the open ocean wave breaking is forced by wind stress and wave–wave interactions. It has not been verified that the aerosol spectra produced are the same in the surf zone, and the open ocean (Lewis and Schwartz, 2004).

Here we present near-surface measurements of aerosol spectra over open ocean whitecaps in the North Atlantic, derive sea spray production fluxes per unit area whitecap, and finally make estimates of the mean surface source fluxes.

2   Measurements

In order to estimate the production of sea spray aerosol from individual wave breaking events, a Compact Lightweight Aerosol Spectrometer Probe (CLASP) (Hill et al., 2008) was mounted on a small buoy with an inlet approximately 1 m above the surface (Fig. 1). The buoy was deployed from the RRS *Discovery* during the two cruises of the Sea Spray, Gas Flux, and Whitecaps (SEASAW) project, part of the UK contribution to the international Surface Ocean Lower Atmosphere Study (SOLAS) (Brooks et al., 2009a, b). The cruises were undertaken in the North Atlantic off the west coast of Scotland and Ireland during the periods 7 November to 2 December 2006 (D313) and 21 March to 12 April 2007 (D317). The buoy is surface following but held in a fixed location, about 8 m from the ship, by a weighted cable suspended from a crane. The wire passes through the buoy's tubular central column, allowing the buoy to ride freely up and down the cable as waves pass it. The weight is held at a depth of roughly 25 m below the ocean surface, beneath the immediate effect of wave motions so as to help restrict sideways movement of the buoy. Power and serial communications to CLASP were provided by a single cable running from the ship.

CLASP provides a 16-channel size spectrum at ambient relative humidity covering the size range $0.12 < R_{amb} < 9.25$ μm at a sample rate of 10 Hz (Hill et al., 2008). The inlet is 0.25 m in length, with one 60 degree bend; particle losses to the walls of the inlet are negligible for particles with radii below 1 μm, 10 % at 3 μm and 20 % at 5 μm. These losses are determined specifically for this inlet and conditions experienced here using the model of Pui et al. (1987) and corrections applied to the spectra. The humidity at 1 m was estimated based on a log profile, using the measured humidity at 21 m and an effective relative humidity at the sea surface of 98 % (Lewis and Schwartz, 2004). Size spectra are subsequently adjusted to 80 % relative humidity via Gerber's (1985) growth model for sea salt.

A video-based bubble measuring system (Leifer et al., 2003a) was mounted on the underside of the buoy, approx-
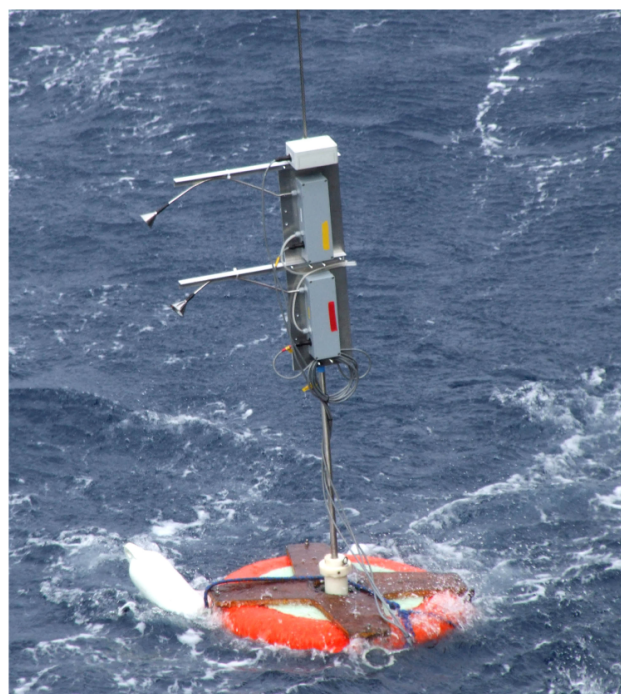

Fig. 1. The tethered buoy. The CLASP units are the two narrow grey boxes; their inlets are visible to the left. The lower unit was damaged and not used in subsequent deployments. The bubble imaging system is mounted below the buoy's floatation ring.

imately 0.4 m below the surface, to make measurements of bubble size spectra in the range $13 < R < 620$ μm. The sample volume ($20 \times 2.9 \times 1.9$ mm³) is imaged by a video camera, illuminated on-axis from directly opposite the camera. Bubbles appear as a dark ring with a brighter surrounding ring and central bright spot. An automated algorithm identifies candidate bubbles, while rejecting other particles such as algae. Full technical details of system and image processing algorithms are given by Leifer et al. (2003a, b). The system has previously been used to examine bubble spectra in both the ocean (de Leeuw and Cohen, 2001; de Leeuw et al., 2003; Norris et al., 2011) and the laboratory (Mårtensson et al., 2003 (MN03 hereafter); Leifer et al., 2003a; Sellegri et al., 2006; Fuentes et al., 2010; Hultin et al., 2010; Zábori et al., 2012). Two minutes of image data were collected at five-minute intervals throughout each deployment. A total of 154 two-minute samples were obtained over 5 successful deployments: 4 during D317 in the open ocean and 1 during D313 in a fetch limited (∼ 5 km) environment behind the Isle of Arran. Each deployment lasted for between one and four hours.

A vertically oriented accelerometer allowed the movement of the buoy over the waves to be determined, along with estimates of the individual wave heights. One-second resolution digital images of the buoy and the surrounding ocean surface were recorded from a webcam on the ship providing a visual check on the buoy and the surface conditions in its immediate

vicinity. Two Nikon CoolPix 8800 digital SLR cameras were installed on the port side of the bridge, approximately 13 m above sea level, from which to estimate the whitecap fraction of breaking waves at the sea surface (Brooks et al., 2009a, b). Images were taken every 30 s during daylight hours. During analysis a portion of each image was selected; this was chosen to exclude the region where the ship's bow wave might be visible, and cropped out the sky and the region of increased brightness close to the horizon. The automated image processing algorithm of Callaghan and White (2009) was used to determine the whitecap fraction for each image. This determines a suitable threshold intensity value for each image with which whitecaps can be separated from the background water. Although effective, the algorithm can fail under some conditions; as a quality control measure each processed image was manually checked to verify its suitability. Images are rejected if they had contamination from sun-glint, sky reflection, birds within the image, or uneven illumination resulting in misidentification of whitecap area by the automated algorithm. Multiple images were averaged to obtain a total of 63 15-min mean whitecap fractions during the periods for which the buoy was deployed.

Mean meteorological conditions were obtained from sensors located on the foremast (see Brooks et al., 2009b for details). One-dimensional wave spectra were obtained from a shipborne wave recorder (SBWR) (Tucker and Pitt, 2001; Holliday et al., 2006). From this wave data the significant wave height, H_s, and mean wave slope (MWS) were calculated. Slopes greater than 0.03 indicate undeveloped sea states; those less than 0.03 indicate well-developed seas (Bourassa et al., 2001). The meteorological and oceanographic conditions during the deployments are summarized in Table 1 and Fig. 2.

3 Results

3.1 Mean aerosol concentrations

The mean aerosol concentration spectra for each deployment are shown in Fig. 3. These are a combination of the background aerosol concentration spectra with the freshly generated aerosol concentration spectra from breaking waves. There is no indication of a systematic wind speed dependence; for $R_{80} < 1\,\mu m$ there is little change in concentration between cases, but the spectra diverge substantially at larger sizes. The persistent concentration of small particles is consistent with their long residence time, while the variability in mean concentration, uncorrelated with wind speed, likely reflects the air mass history. A 30-min long time series of 1-s mean aerosol number concentration from the deployment on 31 March 2007 is shown in Fig. 4. Short periods, typically of the order of a few seconds in duration, have concentrations greater than that for the majority of the record by a factor of 3–7. Comparison of the concentration time series with the
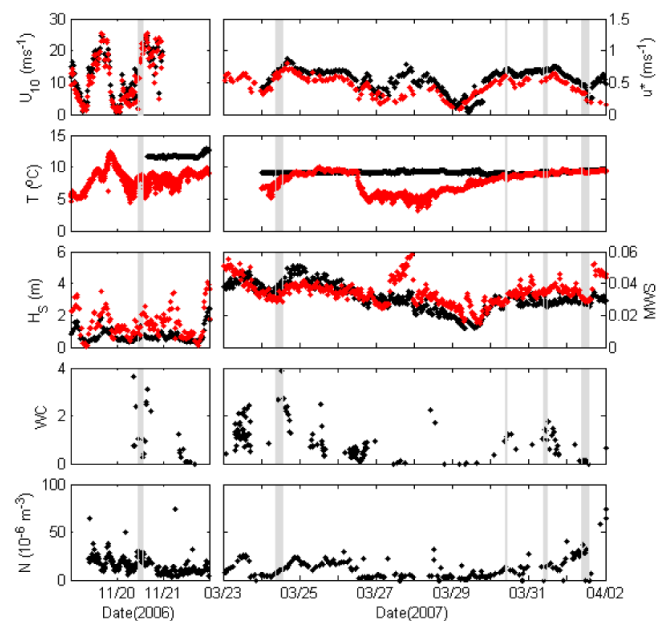

Fig. 2. Time series of mean conditions during the two cruises. Grey shading indicates the times of the buoy deployments. **(a)** 10 m wind speed, U_{10} (m s^{-1}) (black) and friction velocity, u_* (m s^{-1}) (red); **(b)** air temperature at ~ 17 m (red) and near-surface water temperature (black); **(c)** significant wave height H_s (m) (black) and mean wave slope (MWS) (red); **(d)** mean half hourly whitecap coverage WC (%); **(e)** CLASP 28 min averages of particle number concentration (m^{-3}) ($0.12 < R_{80} < 9.25$).

photographic record shows that these peaks in concentration correspond with the occurrence of active whitecaps around the buoy. Only one previous study, that of Wu (1993), has demonstrated the simultaneity of increases in aerosol concentration with breaking wave crests. The source footprint of aerosol reaching the CLASP instrument on the tethered buoy is small, typically about 3 m, estimated using the model of Horst and Weil (1992). This is comparable to the scale of the whitecaps; thus the excess aerosol measured within the concentration peak should be representative of those generated by the whitecap and it should be possible to isolate the spectrum produced by individual whitecaps occurring around the buoy from the mean background spectrum.

A threshold for fresh whitecap aerosol plumes was determined for each individual deployment by applying a 30-point (3-s) running median to the number concentration time series and accepting concentrations greater than two standard deviations above the median. An absolute threshold of approximately double the mean total concentration (N for each deployment) was also applied in order to fully capture plumes lasting longer than three seconds.

Aerosol concentrations greater than the threshold level correspond to fresh plumes over whitecaps and are a mixture of aerosol resulting directly from the whitecap with that of the background; concentrations below the threshold

Table 1. Summary of the meteorological and oceanographic conditions including the 10 m wind speed, U_{10}; friction velocity, u_*; air temperature at 21 m, T_a; relative humidity at 1 m and 21 m; water temperature, T_w; salinity, S; mean wave slope (MWS); significant wave height, H_s; and whitecap fraction, W. The entries in italics are for buoy deployments where bubble spectra were obtained but no aerosol data are available. The deployment date is also shown in Julian Day (JD) format.

| Date	Times	Cruise	U_{10} (m s^{-1})	u_* (m s^{-1})	T_a (°C) 21 m	RH (%) at 1 m	RH (%) at 21 m	T_w (°C)	S (‰)	MWS (m)	H_s (%)	W
20 Nov 2006 JD 324	11:20–13:15	D313	15.1 rising fast	0.69	8.9	92	67.2	11.2	–	0.01	0.98	2.1258
24 Mar 2007 JD 83	09:15–13:15	D317	14.3 rising slowly	0.51	7.6	92	66.4	9.11	35.5	0.031	3.6	1.9163
28 Mar 2007 JD 87	*09:27–11:20*	*D317*	*10.7 steady*	*0.40*	*6.04*	*91*	*63.4*	*9.32*	*35.2*	*0.032*	*2.2*	*2.11*
30 Mar 2007 JD 89	09:00–10:10	D317	14.2 steady	0.50	8.4	95	86.9	9.04	35.5	0.031	3.3	1.143
31 Mar 2007 JD 90	09:17–11:20	D317	14.1 steady	0.49	8.8	97.5	93.2	9.24	35.5	0.035	2.8	1.48
1 Apr 2007 JD 91	09:05–13:30	D317	7.3 slowly falling	0.24	9.3	97.5	93.4	9.39	36.0	0.031	2.8	0.066
4 Apr 2007 JD 94	*13:20–16:30*	*D317*	*10.7 rising*	*0.41*	*11.4*	*94*	*77.8*	*12.3*	*35.5*	*0.028*	*1.8*	*0.45*
5 Apr 2007 JD 95	*09:10–11:41*	*D317*	*11.3 steady*	*0.43*	*11.9*	*95*	*84.5*	*11.6*	*35.5*	*0.032*	*2.4*	*0.49*
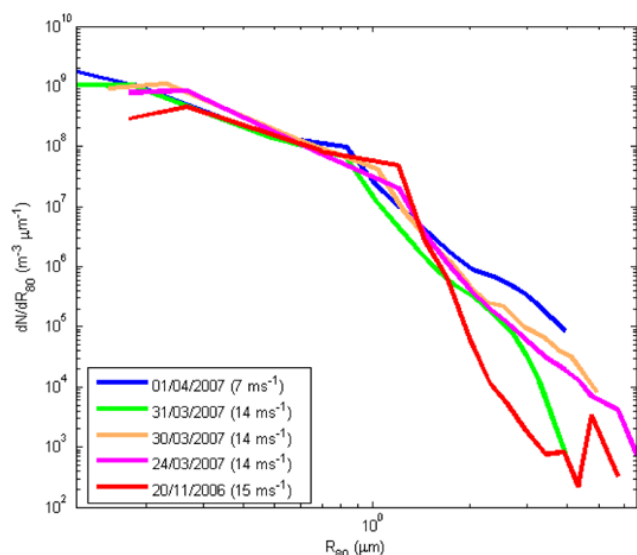
Fig. 3. The mean aerosol concentration spectra for each of the buoy deployments. The deployments are ordered by increasing wind speed, and the same colour scheme, identifying different days, is used throughout all subsequent figures.

represent the ambient background aerosol spectra. The difference between the two provides an estimate of the mean fresh aerosol concentration generated by the whitecaps, dN/dR_{80}.

3.2 Bubble concentrations

Figure 5 shows the mean bubble spectra from each deployment. Also shown for comparison are three other open ocean

spectra (de Leeuw et al., 2003; Phelps and Leighton, 1998; and measurements from DOGEE summarised by Brooks et al., 2009a), two spectra measured in the surf zone (Phelps et al., 1997; Deane and Stokes, 1999), and the MN03 laboratory spectra at water temperatures of 5 °C and 15 °C (measured with the same instrument used here). For completion we have also included bubble spectra from three additional buoy deployments (4, 5 April and 28 March) where there are no corresponding aerosol data available, but were obtained at wind speeds of 10–11 m s^{-1}, lying between those of the other deployments. The mean conditions for these cases are also given in Table 1.

The MN03 bubble spectra were generated in a small container in the laboratory and are clearly not representative of either the surf zone or the open ocean. The bimodal distribution of the MN03 spectra in particular is not observed in any of the natural bubble spectra, and is likely due to the artificial generation. We include them here because, although the bubble spectrum is unrealistic and thus the aerosol production is also unlikely to closely match natural production, the sea spray source function derived from MN03 is used widely in the aerosol modelling community. It is worth noting that the more recent studies of bubble spectra in the laboratory have used weirs (Sellegri et al., 2006) or water jets (Fuentes et al., 2010; Hultin et al., 2010; Zábori et al., 2012) and produce a more realistic open-ocean-like bubble spectra.

For the smallest bubble sizes the concentrations span just over three orders of magnitude across the SEASAW deployments, while for $R > 50\,\mu m$ there is much less variability – about one order of magnitude. The observations shown in Fig. 5 span wind speeds of 5–15 m s^{-1}, and thus large differences in the bubble concentrations and spectral distributions
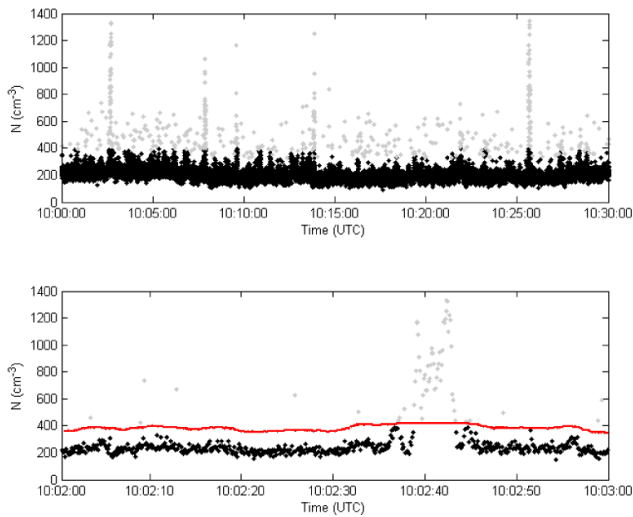
Fig. 4. A 30 min section of the aerosol number concentration (cm^{-3}) ($0.12 < R_{80} < 9.25$) time series (top) and a closer view of 1 min of data (bottom) from the deployment on 31 March. Grey points are the selected whitecap plumes; black points show the ambient background concentration. The red line depicts the threshold.
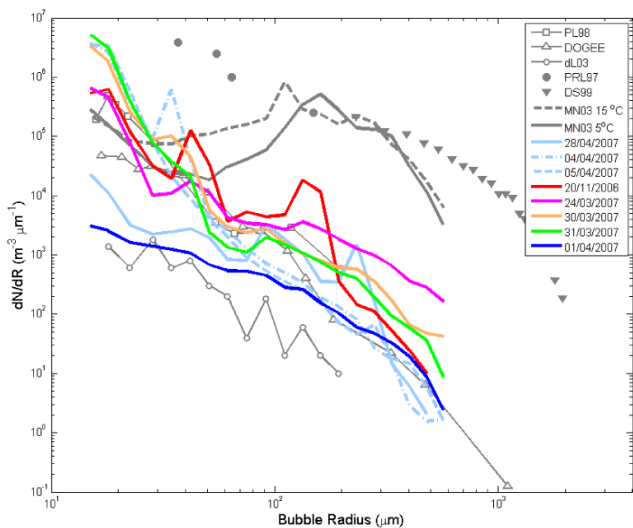

Fig. 5. Mean bubble spectra for each buoy deployment (coloured lines, pale blue lines are cases where no corresponding aerosol measurements are available). A number of previous measurements are shown for comparison (grey lines). The open ocean spectra (open symbols) of de Leeuw et al. (2003) (dL03, $U = 5.8 \, \mathrm{m \, s^{-1}}$), Phelps and Leighton (1998) (PL98, depth 0.5 m, $U = 12 - 14 \, \mathrm{m \, s^{-1}}$), and measurements by Leighton and Coles, summarized in Brooks et al. (2009a) and Pascal et al. (2011) (DOGEE, averaged over a depth of 0–3 m, $U = 13 \, \mathrm{m \, s^{-1}}$), and the surf zone spectra (filled symbols) of Phelps et al. (1997) (PRL97), and Deane and Stokes (1999) (DS99) along with the laboratory bubbles spectra of Mårtensson et al. (2003) at 5 °C (solid grey line) and 15 °C (dashed grey line) are shown for comparison. The Deane and Stokes (1999) measurements are restricted to actively breaking regions of surf.

would be expected. However, although the wind speed is consistent across 24, 30, and 31 March (14.1–14.3 m s^{-1}), there remain significant differences in the bubble spectra; this may result from the variation in wave state between these deployments (Table 1). Significant wave height decreases from 3.6 m on 24 March to 2.8 on 31 March; the concentration for the majority of the bubble spectrum increases with increasing H_s, while that of the smallest bubbles decreases with increasing H_s, the crossover occurring between radii of 25–50 μm. The bubble spectra from 20 November (15 m s^{-1}) have a number of peaks, and the bubble concentration drops off more steeply with increasing bubble size than the other spectra. The ocean conditions were very different on this deployment compared to the three high wind deployments in March 2007 due to the limited fetch of the deployment site, approximately 5 km from the coast. The wave heights were very low with a significant wave height of only 0.98 m compared to ∼ 3 m for the 14 m s^{-1} deployments.

The SEASAW bubble spectra broadly agree with the three other open ocean spectra. All have similar shapes, span a similar range of concentrations and show a similar increase in concentration of the smallest bubbles with increasing wind speed. The surf zone spectra have concentrations 2–3 orders of magnitude higher than the open ocean spectra across the whole measured size range, the difference increasing slightly with increasing size. The MN03 laboratory spectra have concentrations similar to the open ocean spectra for $R < 50 \, \mu\mathrm{m}$, but increase at larger sizes, and match the surf zone spectra for $100 < R < 350 \, \mu\mathrm{m}$.

The variability of individual 2-min estimates of the bubble spectra about the deployment mean is illustrated in Fig. 6 for the cases with one of the highest (31 March, 14 m s^{-1}) and lowest (1 April, 7 m s^{-1}) wind speeds under open ocean conditions. For bubbles smaller than 300 μm, the difference between deployments is much greater than the variability about the deployment mean spectra; for larger bubbles the variability increases significantly – this is due primarily to the occurrence of individual spectral estimates with no bubbles in some of the larger size bins.

Note that the bubble spectra measured here are time averages over the whole deployment and are not restricted to the freshly generated bubble plumes within breaking waves. The other open ocean spectra shown here are similarly time averages; the surf zone spectrum of Phelps et al. (1997) is also a time average, but that of Dean and Stokes (1999) is restricted to the active portion of breaking waves. Within the near-surface layer (depth < 1 m), populations of smaller bubbles have been found to be persistent, varying little over time (Farmer and Vagil, 1989). Leifer et al. (2006) showed that the smallest bubbles ($R < 200 \, \mu\mathrm{m}$) remain in the surface waters after the main body of the plume has surfaced. Bubble terminal rise velocities were calculated following Leifer et al. (2000); they range from 0.0005 m s^{-1} at $R = 15 \, \mu\mathrm{m}$ to 0.14 m s^{-1} at $R = 570 \, \mu\mathrm{m}$ (the largest mean radius measured). The bubble rise velocities suggest that
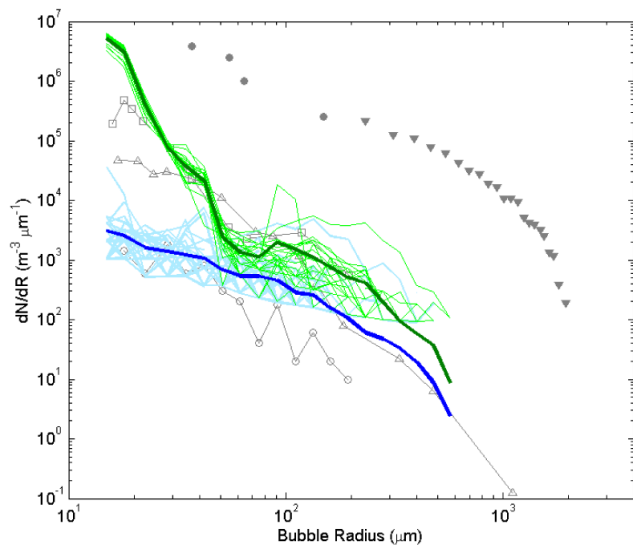
Fig. 6. The mean bubble size spectra (solid lines) for 1 April (7 m s^{-1} winds, blue) and 31 March (14 m s^{-1} winds, green) and all individual measurements from those deployments (pale blue and pale green). Open ocean and surf zone spectra in grey are as in Fig. 5.
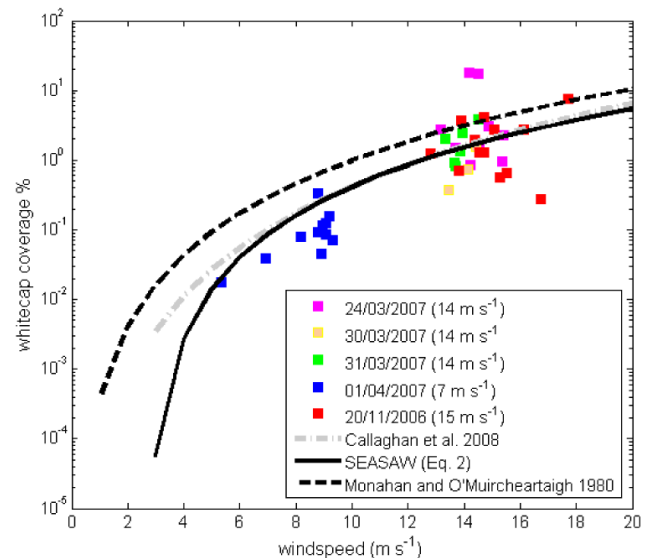

Fig. 7. The SEASAW whitecap estimates during each buoy deployment (symbols), and the whitecap parameterizations from the full SEASAW cruise data set, Callaghan et al. (2008a) and Monahan and O'Muircheartaigh (1980).

bubbles smaller than a few hundred μm can be considered well mixed, with larger bubbles being significantly depleted between wave breaking events. The concentration of bubbles within actively breaking waves will be higher than the mean concentrations measured here, increasingly so with increasing bubble size. The measured spectra are thus not directly representative of those within breaking waves.

3.3 Whitecap coverage

It is well understood that the whitecap fraction on the ocean surface increases with wind speed (Monahan and O'Muircheartaigh, 1980). Figure 7 shows the Monahan and O'Muircheartaigh (1980) parameterisation (Eq. 1) along with that of Callaghan et al. (2008a) and one derived from the measurements obtained during the SEASAW cruises following the method of Monahan and Lu (1990):

$$W = 1.03 \times 10^{-3} (U_{10} - 2.62)^3. \tag{2}$$

The SEASAW whitecap parameterization is very similar to that of Callaghan et al. (2008a) in the wind speed range 8 to 17 m s^{-1} but drops off faster at lower wind speeds. Both are systematically lower than Monahan and O'Muircheartaigh (1980) as are most of the whitecap fraction estimates observed over the last 10 yr (de Leeuw et al., 2011). The 15-min average whitecap fractions for periods matching the bubble spectra estimates during each deployment are also shown in Fig. 7. The overall mean whitecap fractions for each buoy deployment period are given in Table 1. At low wind speeds, 3–5 m s^{-1}, the whitecap parameterizations become problematic; all three of Monahan and

O'Muircheartaigh (1980), Callaghan et al. (2008a) and the SEASAW parameterisations predict low whitecap fractions although they differ by more than an order of magnitude. In practice there are cases where no whitecaps are observed at these low wind speeds.

3.4 Aerosol fluxes

The sea spray source flux, F, is defined here as the product of the particle production flux per unit area of whitecap, F_p, and the whitecap coverage W:

$$\frac{\mathrm{d}F}{\mathrm{d}R_{80}} = W \times \left(\frac{\mathrm{d}F_\mathrm{p}}{\mathrm{d}R_{80}} \right). \tag{3}$$

First we estimate F_p, the particle production flux per unit area whitecap, from the aerosol concentrations. The aerosol concentrations measured on the buoy reflect the net effect of the particle production during the residence time of the air advected past the whitecaps around the buoy. The production flux, F_p, can be estimated as the product of the aerosol number concentration, $\mathrm{d}N/\mathrm{d}R$, with the height of the aerosol plume divided by the residence time of the plume over the whitecap, an approach used by Monahan et al. (1982, 1986). Precise measurements of aerosol plume size and residence time over individual whitecaps are not available, and so we rely here on characteristic scales. A characteristic plume height can be defined as the product of a turbulent velocity scale – the friction velocity u_* – and transit time over the whitecap. The particle production flux is thus estimated simply as the product of excess aerosol number concentration in

Table 2. Summary of the main studies discussed in this paper. Mårtensson et al. (2003), Clarke et al. (2006) and de Leeuw et al. (2000) all use the Monahan and O'Muircheartaigh (1980) whitecap function.

Study	Method	Water T °C	U_{10} m s^{-1}
Mårtensson et al. (2003)	Tank	5 to 25	–
Clarke et al. (2006)	Surf zone	∼ 25	7.3 ± 1.1
de Leeuw et al. (2000)	Surf zone	13 to 18	0 to 9
This study	Open ocean	9 to 11.2	7 to 15

the plume and u_*:

$$\frac{\mathrm{d}F_\mathrm{p}}{\mathrm{d}R_{80}} = \left(\frac{\mathrm{d}N}{\mathrm{d}R_{80}}\right) u_*. \tag{4}$$

The production fluxes for each deployment are shown in Fig. 8, along with production fluxes from MN03, Clarke et al. (2006), and de Leeuw et al. (2000). Conditions for both this and the 3 previous studies are summarised in Table 2. For particles smaller than about 1–2 μm, the SEASAW production fluxes show an increasing trend with wind speed. At $U_{10} = 7$ m s^{-1} the production flux is only slightly higher than that of Clarke et al. (2006), increasing to a factor of 6–7 higher at winds of 14–15 m s^{-1}, but the spectra have a similar slope to those of both Clarke et al. (2006) and de Leeuw et al. (2000). They decrease more rapidly with increasing particle size for $R_{80} > 1$ μm, and for particles with $R_{80} > 2$ μm the production flux falls below those of the previous studies. For these largest particles there is no distinct trend with wind speed. Sea spray source functions based on whitecap fraction usually assume that the production flux is a constant, unaffected by wind speed or the consequent wave state. Here we find both a distinct increase in the total production flux with increasing wind speed, and a change in the shape of the production flux spectra, which steepens with increasing wind speed. Variability in the production flux with wind speed makes physical sense, because the volume of air entrained and depth to which it is injected into the water column will both increase as the size of breaking waves increases.

It is difficult to relate the wind-speed dependence of the production flux directly to the bubble spectra because of the time-averaged nature of the bubble measurements. We note, however, that an increase in production of smaller particles is consistent with an increase in the total volume of air entrained by a breaking wave and consequent increase in the number of large bubbles that rise rapidly to the surface and burst, since these bubbles generate small film drops. The larger aerosols resulting from jet drops are generated by bubbles smaller than about 1 mm (Lewis and Schwartz, 2004); the vast majority of these bubbles are smaller than ∼ 250 μm and will tend to remain within the water column. It is not obvious that an increase in the volume of air entrained by a breaking wave will necessarily result in more small bubbles contributing to the short-duration peak in aerosol measured
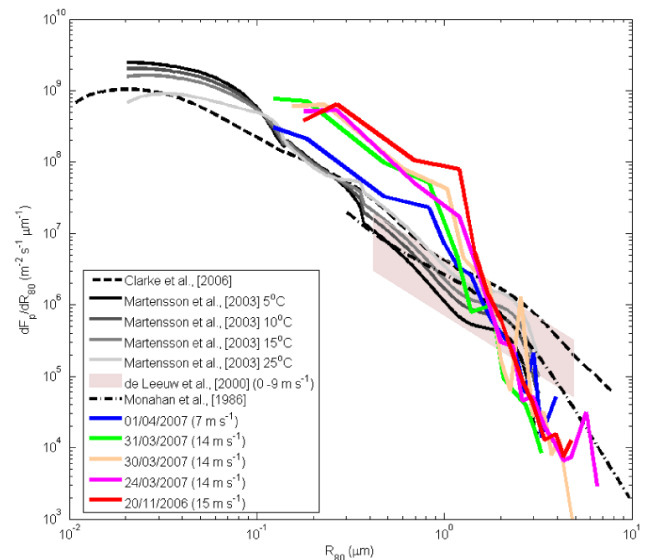

Fig. 8. The mean production flux per unit area of whitecap for each deployment. The production flux functions from previous studies utilizing similar methods are also shown for comparison. The pink shaded area shows the range of the production fluxes estimated by de Leeuw et al. (2000) for a range of wind speeds between 0 and 9 m s^{-1}. The error estimate for the estimated production flux is the same for all the SEASAW deployments: 38.5 %.

directly over an active whitecap. We might, however, expect an increase in the number of small bubbles reaching the surface and bursting over time within the residual foam left after a breaking wave, but these would not be identified by our measurement of the production flux over an active whitecap.

Similar reasoning offers a possible explanation for the differences between the production flux spectra here and those from surf zone studies where the wave breaking process, bubble populations, and bubble plume dynamics are all different from the open ocean case. De Leeuw et al. (2000) estimated the flux from the difference in aerosol concentration on either side of the surf zone under onshore winds, and assumed that production took place throughout the full width of the surf zone. Their production flux is thus an average over active breakers, residual foam between breaking waves, and any foam-free water within the surf zone, and this is likely to be lower than the production flux from actively breaking whitecaps. Clarke et al. (2006) adopted an approach similar to that used here, isolating broad peaks in the aerosol concentration measured upwind of the surf zone, and associating it with individual breaking waves and the residual foam behind them. They estimated the foam fraction between breaking waves and scaled the production flux accordingly. Their production flux is thus an average for active whitecaps and residual foam, and is slightly higher than that of de Leeuw et al. (2000), but again will be lower than that for active whitecaps only. These differences in averaging of source areas can plausibly explain the differences in production flux

for the smaller aerosol, but not the steeper drop-off with size and lower flux obtained here for large particles. We speculate that this may result from differences in wave and bubble plume dynamics between the open ocean and surf zone. The large particles are generated from jet drops, the majority of which result from bubbles small enough to remain within the water column for an extended period of time. In the surf zone, the shallow water column, high turbulence intensity, and more frequent repeated wave breaking mean that these bubbles may be forced back to the surface much more rapidly than in the open ocean, enhancing the production of jet drops and large aerosol. We note that for $R_{80} > 2\,\mu m$ our production flux matches that of Mårtensson et al. (2003) and that their laboratory bubble spectra match our open ocean spectra for the relevant size range, $R < 50\,\mu m$.

Sea spray source fluxes were estimated by scaling the production fluxes with the measured whitecap fractions for each deployment (Eq. 3; Fig. 9); they were also estimated by scaling our production fluxes by both the Monahan and O'Muircheartaigh (1980) and the SEASAW whitecap parameterisations. Also shown in Fig. 9 are a number of other sea spray source functions based on whitecap fraction, and one (Norris et al., 2012) that is derived from direct eddy covariance measurements of the aerosol flux made during the same SEASAW cruise (D317) as most of the buoy measurements presented here. All the previous whitecap-based source functions use the Monahan and O'Muircheartaigh (1980) whitecap parameterisation in their calculations of the fluxes; differences between them thus result solely from differences in their specification of the production flux per unit area whitecap.

There is some indication for a dependence of the sub-micrometer in situ flux estimates on wind history. The recent trend in the wind for each deployment is stated in Table 1. When the wind speed is decreasing slowly (1 April), the in situ source flux matches the other source functions. When it is steady (30 and 31 March), they are on the upper edge of the other source functions. When the wind speed is increasing (24 March) and increasing rapidly (20 November), the in situ source flux is larger than the other source functions by up to an order of magnitude. Similarly, the bubble concentration on 24 March, with rising winds, is higher than on 30 and 31 March, with steady winds of the same speed, $14\,m\,s^{-1}$. Our bubble data set is too limited to draw further conclusions on the effect of wind history. Results from previous studies on the effect of wind history and wave state on wave-breaking and whitecaps are mixed. Several studies find that for a given wind speed the whitecap fraction increases with wave age (the ratio of the phase speed of the peak in the wave spectrum to the wind speed or friction velocity), which implies a reduction in whitecap fraction for rising winds (Sugihara et al., 2001; Callaghan et al., 2008a; Goddijn-Murphy et al., 2011). Callaghan et al. (2008b), however, found a well-defined decrease in whitecap fraction with increasing wave age under fetch-limited conditions, implying higher values in
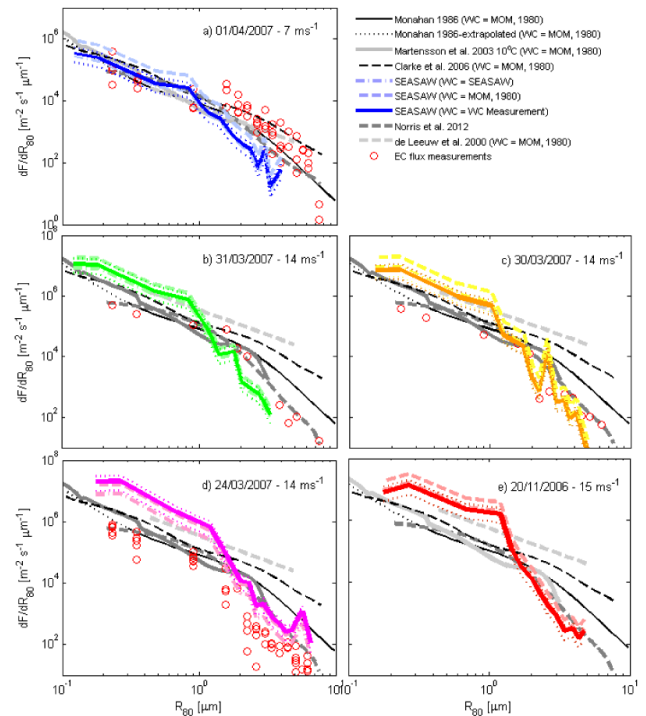

Fig. 9. Mean source fluxes using the production flux estimates (coloured lines) and the measured whitecap fraction (solid lines), and whitecap parameterizations from Monahan and O'Muircheartaigh (1980) (dashed lines) and derived from SEASAW data (dot-dashed lines). The line colours correspond to those used in Figs. 4–7 to identify the deployment date. The dotted lines show the uncertainty around the source flux using the measured whitecap coverage. All other source functions (black and grey lines) use the Monahan and O'Muircheartaigh (1980) (MOM, 1980) whitecap parameterisation. The individual 28-min average eddy covariance aerosol flux measurements made during each of the five deployments are plotted as red circles. N.B. the y-axis scale on **(a)** is shifted relative to the other panels. N.B. the de Leeuw et al. (2000) production flux used is defined at $9\,m\,s^{-1}$, the maximum wind speed in their study (see Table 2) but is applied here up to $15\,m\,s^{-1}$.

increasing winds. This latter case might more closely resemble conditions of rapidly increasing wind in the open ocean, when the wind and waves are far from equilibrium.

Individual eddy covariance (EC) source flux estimates made on the foremast during the periods of the buoy deployments are also shown in Fig. 9. There are no EC data available for 20 November. These EC flux estimates are a subset of those used to formulate the Norris et al. (2012) source function. For particles with $R_{80} < 1\,\mu m$, both the Norris et al. function and the individual fluxes from the EC method are up to 1 order of magnitude below the calculated buoy deployment fluxes except for 1 April. For particles of $R_{80} > 1\,\mu m$ the EC fluxes and the Norris et al. function are just larger than the buoy flux estimate for 1 April; they are within the variability of the buoy estimates for the 30 and 31 March

deployments; but for the 24 March deployment, all the individual EC measurements are lower than any of the other source fluxes. For the lowest wind speed deployment on 1 April, the individual EC fluxes scatter across the full range of the various source functions. Note that the EC estimates, Norris et al. (2012) and both de Leeuw et al. (2000) and Clarke et al. (2006) are effective fluxes at the measurement height, while all others in Fig. 9 are interfacial fluxes; however, for $R_{80} < 10\,\mu m$ interfacial and effective source fluxes differ little and are often assumed to be directly comparable (de Leeuw et al., 2011).

4   Conclusions

Sea spray source fluxes have been estimated from joint in situ measurements of the aerosol produced by individual whitecaps and the fractional coverage of whitecaps in the open ocean of the North Atlantic. Near-surface measurements of aerosol size spectra were made at 1 m above the sea surface from a small tethered buoy, and mean production fluxes estimated per unit area of whitecap. The mean sea spray source flux was then estimated by scaling the whitecap production flux with the observed whitecap fraction. The limited range of wind speeds encountered during the buoy deployments precludes developing a full sea spray source function; however, the results are instructive. Sea spray source fluxes were also estimated by scaling the production flux with two parameterizations of whitecap fraction: Monahan and O'Muircheartaigh (1980) – the most widely used parameterization – and one derived from measurements made during the SEASAW cruises. The in situ whitecap fraction estimates were very scattered, but in general they, and the parameterization derived from the full set of SEASAW whitecap imagery, agree closely with the parameterization of Callaghan et al. (2008b); all of these are significantly lower than the widely used parameterization of Monahan and O'Muircheartaigh (1980).

Bubble size spectra were measured approximately 0.4 m below the surface from the same buoy as the aerosol. The bubble spectra are comparable to previous measurements in the open ocean, and 2–3 orders of magnitude lower than measurements in the surf zone. Note, however, that both our and the previous open ocean measurements cited are time averages, more representative of the persistent background bubble population resulting from wave breaking than of the populations within actively breaking waves. The surf zone measurements include both time-averaged and active breaker bubble spectra; direct comparisons between the two are thus difficult, and some caution should be employed when attempting to infer relationships with aerosol production. The measured bubble concentrations increased with wind speed.

The aerosol production flux per unit area of whitecap derived from mean particle spectra was found to vary with wind speed. For particles with $R_{80} < \sim 1$–$2\,\mu m$, the produc-

tion flux increased with wind speed, while for larger particles there was no clear dependence. The production flux decreased more rapidly with particle size than those of earlier studies. This behaviour is consistent with the observed overall increase in bubble concentrations with wind speed, and implies that a simple single aerosol production flux cannot be defined and scaled by whitecap fraction to determine the mean sea spray source flux. Previous source functions adopting this approach have generally defined a single production flux, often from relatively limited ranges of forcing conditions and none representative of open ocean conditions. Clarke et al. (2006) used surf zone measurements at a single wind speed. De Leeuw et al. (2000) do define a wind-speed–dependent function valid up to $9\,m\,s^{-1}$, but since the measurements are from the surf zone, the physics of the wave breaking is rather different from that in the open ocean.

The mean source flux estimates reflect the production flux results: for $R_{80} < 1\,\mu m$ the flux spectra span the values from previous studies (Monahan et al., 1986; de Leeuw et al., 2000; Mårtensson et al., 2003; Clarke et al., 2006), but decrease more rapidly with increasing size for larger particles. The mean source flux estimates and the EC flux-derived source function of Norris et al. (2012) all decrease more rapidly with increasing particle size than the surf zone functions. This supports the suggestion (Lewis and Schwartz, 2004) that the surf zone is not representative of open ocean whitecapping processes, bubble populations, and aerosol production, since the wave breaking process and bubble plume dynamics are very different for the open ocean and surf zone.

References

Andreas, E. L.: A review of the sea spray generation function for the open ocean, in: Atmosphere-Ocean Interactions, edited by: W. Perrie, 1, 1–46, WIT Press, Southampton, UK, 2002.

Andreas, E. L., Jones, K. F., and Fairall C. W.: Production velocity of sea spray droplets, J. Geophys. Res., 115, C12065, doi:10.1029/2010JC006458, 2010.

Anguelova, M. D. and Webster, F.,: Whitecap coverage from satellite measurements: A first step toward modelling the variability of oceanic whitecaps, J. Geophys. Res., 111, C03017, doi:10.1029/2005JC003158, 2006.

Blanchard, D. C.: The electrification of the atmosphere by particles from bubbles in the sea, Prog. Oceanogr., 1, 171–202, 1963.

Blanchard, D. C.: The oceanic production rate of cloud nuclei, J. Res.-Atmos., 4, 1–6, 1969.

Blanchard, D. C.: The Production, Distribution, and Bacterial Enrichment of the Sea-Salt Aerosol, Air-Sea Exchange of Gases and Particles, edited by: Slinn, W. G. N. and Liss, P. S., Kluwer Academic Publishers, 1983.

Blanchard, D. C.: Surface-active monolayers, bubbles and jet drops, Tellus B, 42, 200–205, 1990.

Blanchard, D. C. and Woodcock, A.: Bubble formation and modification in the sea and its meteorological significance, Tellus, 9, 145–158, 1957.

Bourassa, M. A., Vincent, D. G., and Wood, W. L.: A Sea State Parameterization with Nonarbitrary Wave Age Applicable to Low and Moderate Wind Speeds, J. Phys. Oceanogr., 31, 2840–2851, 2001.

Brooks, I. M., Yelland, M. J., Upstill-Goddard, R. C., Nightingale, P. D., Archer, S., d'Asaro, E., Beale, R., Beatty, C., Blomquist, B., Bloom, A. A., Brooks, B. J., Cluderay, J., Coles, D., Dacey, J., DeGrandpre, M., Dixon, J., Drennan, W. M., Gabriele, J., Goldson, L., Hardman-Mountford, N., Hill, M. K., Horn, M., Hsueh, P.-C., Huebert, B., de Leeuw, G., Leighton, T. G., Liddicoat, M., Lingard, J. J. N., McNeil, C., McQuaid, J. B., Moat, B. I., Moore, G., Neill, C., Norris, S. J., O'Doherty, S., Pascal, R. W., Prytherch, J., Rebozo, M., Sahlee, E., Salter, M., Schuster, U., Skjelvan, I., Slagter, H., Smith, M. H., Smith, P. D., Srokosz, M., Stephens, J. A., Taylor, P. K., Telszewski, M., Walsh, R., Ward, B., Woolf, D. K., Young, D., and Zemmelink, H.: Physical Exchanges at the Air-Sea Interface: Field Measurements from UK-SOLAS, B. Am. Meteorol. Soc., 90, 629–644, doi:10.1175/2008BAMS2578.1, 2009a.

Brooks, I. M., Yelland, M. J., Upstill-Goddard, R. C., Nightingale, P. D., Archer, S., d'Asaro, E., Beale, R., Beatty, C., Blomquist, B., Bloom, A. A., Brooks, B. J., Cluderay, J., Coles, D., Dacey, J., DeGrandpre, M., Dixon, J., Drennan, W. M., Gabriele, J., Goldson, L., Hardman-Mountford, N., Hill, M. K., Horn, M., Hsueh, P.-C., Huebert, B., de Leeuw, G., Leighton, T. G., Liddicoat, M., Lingard, J. J. N., McNeil, C., McQuaid, J. B., Moat, B. I., Moore, G., Neill, C., Norris, S. J., O'Doherty, S., Pascal, R. W., Prytherch, J., Rebozo, M., Sahlee, E., Salter, M., Schuster, U., Skjelvan, I., Slagter, H., Smith, M. H., Smith, P. D., Srokosz, M., Stephens, J. A., Taylor, P. K., Telszewski, M., Walsh, R., Ward, B., Woolf, D. K., Young, D., and Zemmelink, H.: UK-SOLAS Field Measurements of Air-Sea Exchange: Instrumentation, B. Am. Meteorol. Soc., 90, Supplement, 9–16, doi:10.1175/2008BAMS2578.2, 2009b.

Callaghan, A. H. and White, M.: Automated processing of sea surface images for the determination of whitecap coverage, J. Atmos. Ocean. Tech., 26, 383–394. 2009.

Callaghan, A. H., de Leeuw, G., Cohen, L., and O'Dowd, C. D.: Relationship of oceanic whitecap coverage to wind speed and wind history, Geophys. Res. Lett., 35, L23609, doi:10.1029/2008GL036165, 2008a.

Callaghan, A. H., Deane, G. B., and Stokes, M. D.: Observed physical and environmental causes of scatter in whitecap coverage values in a fetch-limited coastal zone, J. Geophys. Res., 113, C05022, doi:10.1029/2007JC004453, 2008b.

Cipriano, R. J., Blanchard, D. C., Hogan, A. W., and Lala, G. G.: On the production of Aitken nuclei from breaking waves and their role in the atmosphere, J. Atmos. Sci., 40, 469–479, 1983.

Cipriano, R. J., Monahan, E. C., Bowyer, P. A., and Woolf, D. K.: Marine condensation nucleus generation inferred from whitecap simulation tank results, J. Geophys. Res., 92, 6569–6576, 1987.

Clarke, A. D., Owens, S. R., and Zhou, J.: An ultra fine sea–salt flux from breaking wave: Implications for cloud condensation nuclei in the remote marine atmosphere, J. Geophys. Res., 111, D06202, doi:10.1029/2005JD006565, 2006.

Day, J. A.: Production of droplets and salt nuclei by the bursting of air bubble films, Q. J. Roy. Meteor. Soc., 90, 72–78, 1964.

Deane, G. B. and Stokes, M. D.: Air entrainment processes and bubble size distributions in the surf zone, J. Phys. Oceanogr., 29, 1393–1403, 1999.

de Leeuw, G.: The occurrence of large salt-water droplets at low-elevations over the open ocean, in: The Climate and Health Implications of Bubble-Mediated Air-Sea Exchange, edited by: Monahan, E. C. and Van Patten, M. A., 65–82, Connecticut Sea Grant College Program CT-SG-89-06, 1989.

de Leeuw, G. and Cohen, L. H.: Bubble size distributions on the North Atlantic and the North Sea in Gas Transfer and water Surfaces, edited by: Donelan, M. A., Drennan, W. M., Salzman, E. S., and Wanninkhof, R., 271–277, AGU, 2001.

de Leeuw, G., Neele, F. P., Hill, M., Smith, M. H., and Vignati, E.,: Production of sea spray aerosol in the surf zone, J. Geophys. Res., 105, 29397–29409, 2000.

de Leeuw, G., Moerman, M., Cohen, L., Brooks, B., Smith, M., and Vignati, E.: Aerosols, bubbles and sea spray production studies during the RED experiments, Proceedings AMS conference, Long Beach, CA, 9–13 February, 2003.

de Leeuw, G., Andreas, E. L., Anguelova, M. D., Fairall, C. W., Lewis, E. R., O'Dowd, C., Schulz, M., and Schwartz S. E.: Production Flux of Sea-Spray Aerosol, Rev. Geophys., 49, RG2001, doi:10.1029/2010RG000349, 2011.

Facchini, M. C., Rinaldi, M., Decesari, S., Carbone, C., Finessi, E., Mircea, M., Fuzzi, S., Ceburnis, D., Flannigan, R., Nilsson, E. D., de Leeuw, G., Martino, M., Woeltjen, J., and O'Dowd, C. D.: Primary submicron marine aerosol dominated by insoluble organic colloids and aggregates, Geophys. Res. Lett., 35, L17814, doi:10.1029/2008GL034210, 2008.

Farmer, D. M. and Vagil, S.: Waveguide propagation of ambient sound in the ocean-surface bubble layer. J. Acoust. Soc. Am., 86, 1897–1908, doi:10.1121/1.398568, 1989.

Fuentes, E., Coe, H., Green, D., de Leeuw, G., and McFiggans, G.: Laboratory-generated primary marine aerosol via bubble-bursting and atomization, Atmos. Meas. Tech., 3, 141–162, doi:10.5194/amt-3-141-2010, 2010.

Georgescu, S.-C., Achard, J., and Canot, E.: Jet drops ejection in bursting gas bubble processes, Eur. J. Mech. B-Fluid., 21, 265–280, 2002.

Gerber, H. E.: Relative-humidity parameterization of the navy aerosol model (NAM), Report No. NRL Report 8956, 17 pp., Navel Research Laboratory, Washington, DC, 1985.

Goddijn-Murphy, L., Woolf, D., and Callaghan, A. H.: Parameterizations and Algorithms for Oceanic Whitecaps, J. Phys. Oceanogr., 41, 741–756, 2011.

Haywood, J. M., Ramaswamy, V., and Soden, B. J.: Tropospheric Aerosol Climate Forcing in Clear-Sky Satellite Observations

over the Ocean, Science, 283, 1299–1303, 1999.

Hill, M. K., Brooks, B. J., Norris, S. J., Smith, M. H., Brooks, I. M., de Leeuw, G., and Lingard, J. J. N.: A Compact Lightweight Aerosol Spectrometer Probe (CLASP), J. Atmos. Ocean. Tech., 25, 1996–2006, doi:10.1175/2008JTECHA1051.1, 2008.

Holliday, N. P., Yelland, M. J., Pascal, R. W., Swail, V. R., Taylor, P. K., Griffiths, C. R., and Kent, E. C.: Were extreme waves in the Rockall Trough the largest ever recorded?, Geophys. Res. Lett., 33, L05613, doi:10.1029/2005GL025238, 2006.

Hoppel, W. A., Frick, G. M., and Fitzgerald, J. W.: The Surface Source Function for Sea-Salt Aerosol and Aerosol Dry Deposition to the Ocean Surface, J. Geophys. Res., 107, 4382–4399, 2002.

Horst, T. W. and Weil, J. C.: Footprint Estimation for Scalar Flux Measurements in the Atmospheric Surface Layer, Bound.-Lay. Meteorol., 59, 279–296, 1992.

Hultin, K. A. H., Nilsson, E. D., Krejci, R., Mårtensson, M., Ehn, M., Hagström, Å., and de Leeuw, G.,: In situ laboratory sea spray production during the Marine Aerosol Production 2006 cruise on the northeastern Atlantic Ocean, J. Geophys. Res., 115, D06201, doi:10.1029/2009JD012522, 2010.

Johnson, B. D. and Wangersky, P. J.: Microbubbles: Stabilization by monolayers of adsorbed particles, J. Geophys. Res., 92, 14641–14647, 1987.

Keene, W. C., Maring, H., Maben, J. R., Kieber, D. J., Pszenny, A. A. P., Dahl, E. E., Izaguirre, M. A., Davis, A. J., Long, M. S., Zhou, X., Smoydzin, L, and Sander, R.: Chemical and physical characteristics of nascent aerosols produced by bursting bubbles at a model air sea interface, J. Geophys. Res., 112, D21202, doi:10.1029/2007JD008464, 2007.

Kolovayev, P. A.: Investigation of the concentration and statistical size distribution of wind-produced bubbles in the near-surface ocean layer, Oceanology, 15, 659–661, 1976.

Leifer, I., Patro, R. K., and Bowyer, P.: A study on the temperature variation of rise velocity for large clean bubbles, J. Atmos. Ocean. Tech., 17, 1392–1402, 2000.

Leifer, I., de Leeuw, G., and Cohen, L. H.: Optical Measurement of Bubbles: System Design and Application. J. Atmos. Ocean. Tech., 20, 1317–1332, 2003a.

Leifer, I., de Leeuw, G., Kunz, G., and Cohen, L. H.: Calibrating optical bubble size by the displaced mass method, Chem. Eng. Sci., 58, 5211–5216, 2003b.

Leifer, I., Caulliez, G., and de Leeuw, G.: Bubbles generated from wind-steepened breaking waves: 2. Bubble plumes, bubbles, and wave characteristics, J. Geophys. Res., 111, C06021, doi:101029/2004JC002676 2006.

Leighton, T. G. and Robb, G. B. N.,: Preliminary mapping of void fractions and sound speeds in gassy marine sediments from subbottom profiles, J. Acoust. Soc. Am., 124, EL313–EL320, 2008.

Lewis, E. R. and Schwartz, S. E.,: Sea Salt Aerosol Production – Mechanisms, Methods, Measurements, and Models, American Geophysical Union, 2004.

Mårtensson, E. M., Nilsson, E. D., de Leeuw, G., Cohen, L. H., and Hansson, H. C.: Laboratory simulations and parameterization of the primary marine aerosol production, J. Geophys. Res., 108, 4297, 2003.

Medwin, H.: In situ acoustic measurements of bubble populations in coastal waters, J. Geophys. Res., 75, 599–611, 1970.

Monahan, E. C.: Sea Spray as a function of low elevation wind speed, J. Geophys. Res., 73, 1127–1137, 1968.

Monahan, E. C.: Oceanic whitecaps, J. Phys. Oceanogr., 1, 139–144, 1971.

Monahan, E. C. and Lu, M., : Acoustically relevant bubble assemblages and their dependence on meteorological parameters, IEEE J. Oceanic Eng., 15, 340–349, 1990.

Monahan, E. C. and O'Muircheartaigh, I.: Optimal Power-Law Description of Oceanic Whitecap Coverage Dependence on Wind Speed, J. Phys. Oceanogr., 10, 2094–2099, 1980.

Monahan, E. C. and O'Muircheartaigh, I.: Review Article: Whitecaps and the Passive Remote Sensing of the Ocean Surface, Int. J. Remote Sens., 7, 627–642, 1986.

Monahan, E. C., Spiel, D. E., and Davidson, K. L.,: Whitecap aerosol productivity deduced from simulation tank measurements, J. Geophys. Res., 87, 8898–8904, 1982.

Monahan, E. C., Spiel, D. E., and Davidson, K. L.: A model of marine aerosol generation via whitecaps and wave disruption, in: Oceanic Whitecaps, edited by: Monahan, E. C. and Mac Niocaill, G. D., Reidel Publishing Company, 167–174, 1986.

Morelli, J., Buat-Menard, P., and Chesselet, R.,: Production experimentale d'aerosols a la surface de la mer, J. Res.-Atmos., 8, 961–986, 1974.

Norris, S. J., Brooks, I. M., de Leeuw, G., Sirevaag, A., Leck, C., Brooks, B. J., Birch, C. E., and Tjernström, M.: Measurements of bubble size spectra within leads in the Arctic summer pack ice, Ocean Sci., 7, 129–139, doi:10.5194/os-7-129-2011, 2011.

Norris, S. J., Brooks, I. M., Hill, M. K., Brooks, B. J., Smith, M. H., and Sproson, D. A. J.: Eddy Covariance Measurements of the Sea Spray Aerosol Flux over the Open Ocean, J. Geophys. Res., 117, D07210, doi:10.1029/2011JD016549, 2012.

O'Dowd, C. D., Lowe, J. A., and Smith, M. H.,.: Coupling of sea-salt and sulphate interactions and its impact on cloud droplet concentration predictions, Geophy. Res. Lett., 26, 1311–1314, 1999.

O'Dowd, C. D., Lowe, J. A., Clegg, N., Smith, M. H., and Clegg, S. L.: Modelling heterogeneous sulphate production in maritime straiform clouds. J. Geophys. Res., 105, 7143–7160, 2000.

Pascal, R. W., Yelland, M. J., Srokosz, M. A., Moat, B. I., Waugh, E. M., Comben, D. H., Clansdale, A. G., Hartman, M. C., Coles, D. G. H., Ping-Chang Hsueh, and Leighton, T. G.: A spar buoy for high frequency wave measurements and detection of wave breaking in the open ocean, J. Atmos. Ocean. Tech., 28, 590–605, 2011.

Parameswaran, K.: Influence of micrometeorological features on coastal boundary layer aerosol characteristics at the tropical station, Trivandrum, J. Earth Syst. Sci., 110, 247–265, 2001.

Phelps, A. D. and Leighton, T. G.,: Oceanic bubble population measurements using a buoy-deployed combination frequency technique, IEEE J. Oceanic Eng., 23, 400–410, 1998.

Phelps, A. D., Ramble, D. G., and Leighton, T. G.: The use of a combination frequency technique to measure the surf zone bubble population, J. Acoust. Soc. Am., 101, 1981–1989, 1997.

Pui, D. Y. H., Romay-Novas, F., and Lui, B. Y. H.: Experimental study of particle deposition in bends of circular cross section, Aerosol Sci. Tech., 7, 301–315, 1987.

Sellegri, K., O'Dowd, C. D., Yoon, Y. J., Jennings, S. G., and de Leeuw. G.,: Surfactants and submicron sea spray generation, J. Geophys. Res., 111, D22215, doi:10.1029/2005JD006658, 2006.

Spiel, D. E.: A study of aerosols generated in a whitecap simulation tank, BDM Tech, Rep. 006-83, Monterey, 35 pp., 1983.

Spiel, D. E.: The sizes of the jet drops produced by air bubbles bursting on sea and fresh-water surfaces, Tellus B, 46, 325–338, 1994.

Spiel, D. E.: A hypothesis concerning the peak in film drop production as a function of bubble size. J. Geophys. Res., 102, 1153–1161, 1997.

Sugihara, Y. H., Tsumori, T., Ohga, T., Yoshioka, H., and Serizava, S.: Variation of whitecap coverage with wave-field conditions, J. Marine Syst., 66, 47–60, 2007.

Tucker, M. J. and Pitt, E. G.,.: Waves in Ocean Engineering, Ocean Eng. Book Ser., 5, Elsevier, New York, 521 pp., 2001.

Tyree, C. A., Hellion, V. M., Alexandrova, O. A., and Allen, J. O.: Foam droplets generated from natural and artificial seawaters, J. Geophys. Res., 112, D12204, doi:10.1029/2006JD007729, 2007.

Wettlaufer, G.: Introduction to crystallization phenomena in natural and artificial sea ice, in: The Physics of ice covered seas, edited by: Lepparantä, M., Univ. of Helsinki, Helsinki, 105–195, 1998.

Woodcock, A. H., Blanchard, D. C., and Rooth, C. G. H.: Salt-induced convection and clouds, J. Atmos. Sci., 20, 159–169, 1963.

Woolf, D. K., Monahan, E. C., and Spiel, D. E.,: Quantification of the marine aerosol produced by whitecaps, in: Seventh Congress on Ocean – Atmosphere Interaction, 182–185, American Meteorological Society, Anaheim, CA, 1988.

Wu, J.: Production of spume drops by the wind tearing of wave crests: The search for quantification, J. Geophys. Res., 98, 18221–18227, 1993.

Wu, J., Murray, J. J., and Lai, R. J.: Production and distributions of sea spray, J. Geophys. Res., 89, 8163–8169, 1984.

Zábori, J., Krejci, R., Ekman, A. M. L., Mårtensson, E. M., Ström, J., de Leeuw, G., and Nilsson, E. D.: Wintertime Arctic Ocean sea water properties and primary marine aerosol concentrations, Atmos. Chem. Phys., 12, 10405–10421, doi:10.5194/acp-12-10405-2012, 2012.